Differ Equ Dyn Syst (2012) 20:339–366
DOI 10.1007/s12591-012-0142-6

ORIGINAL RESEARCH

Bifurcation Analysis and Control of Leslie–Gower Predator–Prey Model with Michaelis–Menten Type Prey-Harvesting

R. P. Gupta · Malay Banerjee · Peeyush Chandra

Published online: 3 August 2012

Abstract In this paper, a bi-dimensional system of ordinary differential equation prey–predator model with nonlinear prey-harvesting is analyzed. The model is a modified version of the well known Leslie–Gower type prey–predator model. The original Leslie–Gower type model has the unique interior equilibrium point which is globally asymptotically stable. We show here that the nonlinear harvesting in prey significantly modifies the dynamics of the system in comparison to the proportionate harvesting of prey. It has been observed that the system goes to extinction for a wide range of initial values. Moreover, the model can have two, one or no interior equilibrium point in the first quadrant where two interior equilibria collapse to one interior equilibrium point and then disappear through saddle-node bifurcation considering the rate of harvesting as bifurcation parameter. The local existence of limit cycle appearing through local Hopf bifurcation and its stability have also been investigated by computing first Lyapunov number. The conditions for existence of bionomic equilibria are analyzed. Pontryagin's Maximum Principle is used to characterize the optimal singular control. Numerical examples are provided to validate our findings.

Keywords Stability · Phase portraits · Bifurcations · Bionomic equilibria · Singular optimal control

Introduction

In recent times, the growing need for more food and resources has led to an increased exploitation of several biological resources. There is also a global concern to protect the ecosystem at large. In the face of these two opposing approaches, we are now-a-days looking for a sustainable development policy in almost every sphere of human activity. This has necessitated a scientific management of commercial exploitation of the biological resources like fisheries and forestries. Predator–prey system is one of the most important population models, which

R. P. Gupta · M. Banerjee (✉) · P. Chandra
Department of Mathematics and Statistics, IIT, Kanpur 208 016, India
e-mail: malayb@iitk.ac.in

has received extensive attention from harvesting and optimal management of natural resource point of view. The dynamic relationship between predators and their prey has been and will continue to be one of the dominant themes in mathematical ecology due to its universal existence and importance [7].

Effects of harvesting in various types of prey–predator models have been considered by many researchers. Mathematical modeling with harvesting of renewable resources started with the studies of Clark [3,4]. The problem of combined harvesting of two ecologically independent and logistically growing fish species was studied by Clark [3]. Brauer and Soudack [1,2] developed a predator–prey system with constant rate harvesting in prey and studied its dynamical behavior. They also elaborated that the presence of harvesting reduces the region of asymptotic stability in the predator–prey plane. Zhang et al. [23] studied the problem of combined harvesting of prey–predator model with prey reserve by considering different harvesting effort. Rojas-Palma and González-Olivares [20] described an open access fishery of the predator–prey type where the functional response of the predators is of Holling type-III and the prey growth is affected by the Allee effect in which both prey and predator species are subjected to non-selective harvesting based on the catch per unit effort (CPUE) (i.e. Schefer's hypothesis). Leard et al. [14] considered Michaelis–Menten type ratio-dependent predator–prey model with a density dependent harvesting of prey while Lenzini and Rebaza [15] studied a ratio-dependent prey–predator model by taking a non-constant harvesting in predator. A Leslie–Gower predator–prey model incorporating harvesting has been studied by Zhang et al. [24]. They showed that the unique positive equilibrium of the system is globally stable, which means that suitable harvesting has no influence on the persistent property of the harvesting system. They further showed that harvesting has no influence on the ultimate density of the prey species while the density of predator species strictly decreases with the harvesting effort.

There are basically three types of harvesting reported in the literature (i) constant harvesting where a constant number of individuals are harvested per unit of time, (ii) proportional harvesting $h(x) = qEx$ that means the number of individuals harvested per unit of time is proportional to the current population and (iii) nonlinear harvesting $H(x) = qEx/(m_1E + m_2x)$ (Holling type-II), where q is the catchability coefficient, E is the effort applied to harvest individuals which is measured in terms of number of (standard) vessels being used to harvest the individual population and m_1, m_2 are suitable positive constants. It has been noticed that the proportionate harvesting embodies several unrealistic features like (i) random search for prey, (ii) equal likelihood of being captured for every prey species, (iii) unbounded linear increase of $h(x)$ with x for fixed E and unbounded linear increase of $h(x)$ with E for fixed x [5]. The functional form $H(x) = qEx/(m_1E + m_2x)$ is more realistic in the sense that the above unrealistic features are largely removed. It may be noted that $H(x) \to qE/m_2$ as $x \to \infty$ and $H(x) \to qx/m_1$ as $E \to \infty$. This shows that the nonlinear harvesting function exhibits saturation effects with respect to both the stock abundance and the effort-level. Also the parameter m_1 is proportional to the ratio of the stock-level to the harvesting rate (catch-rate) at higher levels of effort and m_2 is proportional to the ratio of the effort-level to the harvesting rate (catch-rate) at higher stock-levels.

Zhu and Lan [25] studied Leslie–Gower model with constant harvesting in prey. They studied phase portraits near these positive equilibria. They also proved that the predator free equilibria are saddle-nodes, saddles or unstable nodes depending on the choices of the parameters involved while the interior positive equilibria in the first quadrant are saddles, stable or unstable nodes, foci, centers, saddle-nodes or cusps. The dynamics of Leslie–Gower model with proportionate harvesting is almost similar to the original Leslie–Gower model except some modifications in parameters which has been studied by Mena-Lorca et al. [17].

Though there are numerous works on predator–prey system incorporating the harvesting, Leslie–Gower predator prey model under the assumption of the nonlinear harvesting on prey species has not been studied. Therefore we consider the Leslie–Gower model with the nonlinear harvesting in prey. We have analyzed this model for its global dynamics and singular optimal control.

Mathematical Model

Basic Model

The Leslie–Gower type model described by the autonomous bi-dimensional system of differential equations [7] in extended form is given by:

$$\begin{cases} \frac{dx}{dt} = \left(r\left(1-\frac{x}{K}\right)-\alpha y\right)x, \\ \frac{dy}{dt} = s\left(1-\frac{y}{nx}\right)y, \quad \text{if } (x,y)\neq(0,0) \\ \frac{dy}{dt} = 0, \quad \text{if } (x,y)=(0,0), \end{cases} \tag{1}$$

subjected to positive initial conditions $x(0) > 0,\ y(0) > 0$. Here, $x \equiv x(t)$ and $y \equiv y(t)$, are the prey and predator population densities respectively.
System (1) is defined on the set:

$$\Omega = \{(x,y) \in \mathbb{R}^2 | x \geq 0, y \geq 0\} = \mathbb{R}_0^+ \times \mathbb{R}_0^+, \tag{2}$$

with all the parameters r, K, α, s and n being positive. Further, the parameters have the following biological meanings:

(i) r and s are intrinsic growth rates or biotic potential of the prey and predators, respectively.
(ii) K is the environmental carrying capacity for prey.
(iii) α is the maximal predator per capita consumption rate.
(iv) n is a measure of food quality that the prey provides towards the predator births.

Here the interaction between prey and predator is expressed by the Holling type-I (linear) functional response [10] that is $f(x) = \alpha x$. Further the subsistence of predator depends exclusively on prey population hence the conventional environmental carrying capacity K_y of predator is taken to be proportional to prey abundance x, thus $K_y = n\,x$ [22].

In [17], it is shown that apart from the axial equilibrium point $(K, 0)$ the system (1) has a unique interior equilibrium point (x_e, nx_e) where $x_e = \frac{rK}{r+K\alpha n}$, which is globally asymptotically stable. Thus they concluded that the quantity of predators at the equilibrium depends directly on the quantity of prey at equilibrium multiplied by the food quality that the prey offers. If it is of good quality ($n \to \infty$), more predator can survive and require less quantity of prey and if it is of bad quality, less predators will be born. On the other hand, in absence of predators, prey quantity in equilibrium is K as in this case the axial equilibrium $(K, 0)$ becomes globally stable.

The Model with Prey Harvesting

As mentioned in the "Introduction", the nonlinear harvesting $H(x) = qEx/(m_1E + m_2x)$ is more realistic therefore in this paper we consider Leslie–Gower prey–predator model with

nonlinear harvesting. In view of this the above model modifies to the following autonomous system of differential equations:

$$\begin{cases} \frac{dx}{dt} = \left(r\left(1-\frac{x}{K}\right) - \alpha y - \frac{qE}{m_1E+m_2x}\right)x, \\ \frac{dy}{dt} = s\left(1-\frac{y}{nx}\right)y, \quad \text{if } (x,y) \neq (0,0) \\ \frac{dy}{dt} = 0, \quad \text{if } (x,y) = (0,0), \end{cases} \tag{3}$$

subjected to positive initial conditions $x(0) > 0,\ y(0) > 0$. The parameters r, K, α, s, n have the same biological meaning as in the model (2), q is the catchability coefficient, E is the effort applied to harvest individuals and m_1, m_2 are suitable constants. All the parameters are assumed to be positive. The system (3) is defined on the set $\mathbb{R}_0^+ \times \mathbb{R}_0^+$.

In order to investigate the dynamics of system (3) we will consider the following dimensionless parameters

$$x = Ku, \quad y = nKv, \quad rt = \tau, \quad b = \frac{\alpha nK}{r}, \quad c = \frac{m_1E}{m_2K}, \quad h = \frac{qE}{rm_2K}, \quad \rho = \frac{s}{r}. \tag{4}$$

Using above transformations we obtain the following system of differential equations involving four dimensionless parameters:

$$\begin{cases} \frac{du}{d\tau} = \left(1-u-bv-\frac{h}{c+u}\right)u \equiv uf^{(1)}(u,v), \\ \frac{dv}{d\tau} = \rho v\left(1-\frac{v}{u}\right) \equiv vf^{(2)}(u,v), \quad \text{if } (u,v) \neq (0,0) \\ \frac{dv}{d\tau} = 0, \quad \text{if } (u,v) = (0,0), \end{cases} \tag{5}$$

with the initial conditions

$$u(0) = u_0 > 0,\ v(0) = v_0 > 0. \tag{6}$$

Here

$$f^{(1)}(u,v) = 1-u-bv-\frac{h}{c+u}, \quad f^{(2)}(u,v) = \rho\left(1-\frac{v}{u}\right) \tag{7}$$

and b, c, h and ρ are all positive.

Positivity and Boundedness of Solutions

Lemma 1 *(a) All solutions $(u(\tau), v(\tau))$ of the system (5) with the initial condition (6) are positive, i.e., $u(\tau) > 0, v(\tau) > 0$, for all $\tau \geq 0$.*

(b) All solutions $(u(\tau), v(\tau))$ of the system (5) with the initial condition (6) are bounded, for all $\tau \geq 0$.

Proof (a) Integrating Eq. (5) with initial conditions (6), we have

$$u(\tau) = u_0 \exp\left(\int_0^\tau f^{(1)}(u(s), v(s))ds\right) > 0,$$

$$\text{and} \quad v(\tau) = v_0 \exp\left(\int_0^\tau f^{(2)}(u(s), v(s))ds\right) > 0.$$

Hence all solutions starting in

$$Int(\Omega) = \{(u, v) \in \mathbb{R}^2 \mid u > 0, v > 0\},$$

remain in $Int(\Omega)$ for all $\tau \geq 0$.

Also, if any trajectory starts on positive direction of u-axis then it remains on it at all future time and hence positive u-axis is an invariant set for the system (5). Similarly positive v-axis is also an invariant set. Combining these results we observe that the set Ω defined in (2) is invariant set for the system (5).

(b) Now, to prove the boundedness of solutions of system (5) with the initial condition (6), we use the positivity of variables u, v and Lemma 2.2 of [16]. From (5) we can write

$$\frac{du}{d\tau} = \left(1 - u - bv - \frac{h}{c+u}\right) u \leq u(1-u),$$

therefore,

$$u(\tau) \leq \max\{1, u_0\} \equiv M_1.$$

Further, from (5) we have

$$\frac{dv}{d\tau} = \rho v \left(1 - \frac{v}{u}\right) \leq \rho v \left(1 - \frac{v}{M_1}\right),$$

therefore,

$$v(\tau) \leq \max\{M_1, v_0\} \equiv M_2.$$

This completes the proof of the boundedness of solutions and hence the system under consideration is a dissipative system. □

Existence, Stability and Bifurcation of Equilibria

In order to find the equilibrium points of the system (5), we need to study the shape and location of zero growth isoclines of the system (5) as equilibrium points are their points of intersection. The system (5) has equilibrium point at (0, 0) and others are obtained by

$$f^{(1)}(u, v) = 0, \quad v f^{(2)}(u, v) = 0.$$

The axial equilibrium point are given by the roots of the quadratic equation

$$u^2 - (1-c)u + h - c = 0 \tag{8}$$

and the interior equilibria are given by the roots of the following quadratic equation

$$(b+1)u^2 - (1 - c(b+1))\, u + h - c = 0. \tag{9}$$

The roots of the two Eqs. (8) and (9) depend on the parameters h and c, so we shall consider the following cases.

Case-I: $h > c$

Axial Equilibria

The possible equilibrium points on the boundary of first quadrant for the system (5) are:

$$E_L = (u_L, 0), \quad E_H = (u_H, 0),$$

where u_L and u_H are the positive real roots of the quadratic Eq. (8) with $u_L < u_H$ and are given by

$$u_L = \frac{1 - c - \sqrt{(1-c)^2 - 4(h-c)}}{2} \text{ and } u_H = \frac{1 - c + \sqrt{(1-c)^2 - 4(h-c)}}{2}. \quad (10)$$

The two real positive roots u_L and u_H will exist if $c < 1$ and $(1-c)^2 - 4(h-c) > 0$. Note that the other cases are not biologically feasible.

Interior Equilibria

In order to find the interior equilibrium points we solve the equations

$$(1-u)(c+u) - bv(c+u) - h = 0 \text{ and } u = v, \quad (11)$$

by eliminating v to get the quadratic Eq. (9). The two real roots of the Eq. (9) are given by

$$u_{1*} = \frac{1}{2(b+1)}\left(1 - c(b+1) - \sqrt{(1-c(b+1))^2 - 4(b+1)(h-c)}\right) \quad (12)$$

and

$$u_{2*} = \frac{1}{2(b+1)}\left(1 - c(b+1) + \sqrt{(1-c(b+1))^2 - 4(b+1)(h-c)}\right). \quad (13)$$

The interior equilibrium points $E_{1*}(u_{1*}, u_{1*})$ and $E_{2*}(u_{2*}, u_{2*})$ are feasible if

$$c(b+1) < 1 \text{ and } (1-c(b+1))^2 - 4(b+1)(h-c) > 0.$$

Further if $(1-c(b+1))^2 - 4(b+1)(h-c) = 0$, then both the roots u_{1*} and u_{2*} coincide and hence we get one interior equilibrium point $\bar{E}(\bar{u}, \bar{u})$ where

$$\bar{u} = \frac{1 - c(b+1)}{2(b+1)}.$$

The number of interior equilibrium points are shown in the Fig. 1 for different values of h with rest of the parameters fixed.

Remark 1 Whenever there exist two different axial and two different interior equilibrium points then (a) $0 < u_L < u_H < 1$ and (b) $0 < u_{1*} < u_{2*} < 1$.

Stability of Equilibria

Theorem 1 *(a) The equilibrium point $E_L = (u_L, 0)$ is repeller and (b) $E_H = (u_H, 0)$ is always a saddle point.*

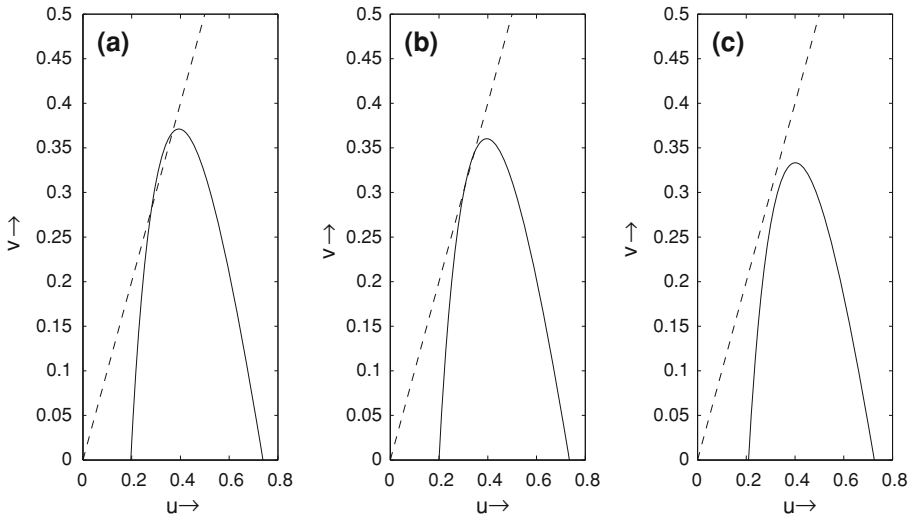

Fig. 1 Number of interior equilibrium point for $b = 0.400$, $c = 0.065$ depends solely upon h; **a** $h = 0.210$, two interior equilibrium points, **b** $h = 0.212$, unique instantaneous interior equilibrium point and **c** $h = 0.217$, no interior equilibrium point. Here *dashed line* is predator nullcline and *solid curve* is prey nullcline.

Proof The Jacobian of the system (5) evaluated at a point $(u, 0)$ is

$$M = \begin{pmatrix} \beta_{11} & -bu \\ 0 & \rho \end{pmatrix},$$

where $\beta_{11} = 1 - 2u - \frac{hc}{(c+u)^2}$.
The eigenvalues of the matrix M are β_{11} and ρ. Clearly ρ is positive so we look for the sign of β_{11}.

(a) At the equilibrium point $E_L = (u_L, 0)$, we have

$$\beta_{11} = 1 - 2u_L - \frac{hc}{(c+u_L)^2},$$

using (8) and (10), we get

$$\beta_{11} = 1 - 2u_L - \frac{c(1-u_L)}{c+u_L} \equiv \frac{u_L\sqrt{(1-c)^2 - 4(h-c)}}{c+u_L} > 0.$$

Therefore, $E_L = (u_L, 0)$ is a repeller as both the eigenvalues of the Jacobian matrix are positive.

(b) Similarly, at the point $E_H = (u_H, 0)$, we have

$$\beta_{11} = -\frac{u_H\sqrt{(1-c)^2 - 4(h-c)}}{c+u_H} < 0.$$

Thus the two eigenvalues are of opposite signs hence $E_H = (u_H, 0)$ is a saddle point.

Theorem 2 *(a) The equilibrium point $E_{1*}(u_{1*}, u_{1*})$ is a saddle point.*
(b) $E_{2*}(u_{2*}, u_{2*})$ is locally asymptotically stable if $(2+b){u_{2*}}^2 + (\rho + c - 1)u_{2*} + \rho c > 0$.
(c) The system undergoes a Hopf bifurcation with respect to bifurcation parameter ρ around the equilibrium point $E_{2*}(u_{2*}, u_{2*})$ if $(2+b){u_{2*}}^2 + (\rho + c - 1)u_{2*} + \rho c = 0$.

Proof The Jacobian of the system (5) evaluated at the point (u, u) is

$$N = \begin{pmatrix} c_{11} & -bu \\ \rho & -\rho \end{pmatrix},$$

where, $c_{11} = 1 - (2+b)u - \dfrac{hc}{(c+u)^2}$.

(a) For E_{1*},

$$\det N|_{E_{1*}} = -\rho\left(1 - 2(b+1)u_{1*} - \frac{hc}{(c+u_{1*})^2}\right),$$

from (9), we get

$$\det N|_{E_{1*}} = -\rho\left(1 - 2(b+1)u_{1*} - \frac{c(1-u_{1*}-bu_{1*})}{c+u_{1*}}\right).$$

Now using the expression for u_{1*} from (12) and Eq. (9), we get

$$\det N|_{E_{1*}} = -\frac{\rho u_{1*}}{c+u_{1*}}\sqrt{(1-c(b+1))^2 - 4(b+1)(h-c)} < 0.$$

Hence from Routh-Hurwitz criterion $E_{1*}(u_{1*}, u_{1*})$ is a saddle point.

(b) Now for E_{2*},

$$trN|_{E_{2*}} = 1 - (b+2)u_{2*} - \frac{hc}{(c+u_{2*})^2} - \rho,$$

and using Eq. (9), we get

$$trN|_{E_{2*}} = -\frac{1}{c+u_{2*}}\left((2+b){u_{2*}}^2 + (\rho+c-1)u_{2*} + \rho c\right).$$

Further,

$$\det N|_{E_{2*}} = -\rho\left(1 - 2(b+1)u_{2*} - \frac{c(1-u_{2*}-bu_{2*})}{c+u_{2*}}\right),$$

substituting the expression for u_{2*} from (13) and using Eq. (9), we get

$$\det N|_{E_{2*}} = \frac{\rho u_{2*}}{c+u_{2*}}\sqrt{(1-c(b+1))^2 - 4(b+1)(h-c)} > 0.$$

Hence result follows from Routh-Hurwitz criterion.

(c) We know that if the $trN|_{E_{2*}} = 0$, then both the eigenvalues will be purely imaginary provided $\det N|_{E_{2*}} > 0$. Therefore, the implicit function theorem says that a Hopf bifurcation occurs where a periodic orbit is created as the stability of the equilibrium point $E_{2*}(u_{2*}, u_{2*})$ changes. Note that $trN|_{E_{2*}} = 0$ gives the Hopf bifurcation point $\rho = \rho^{[hf]}$. Further from part (b) it is clear that under the given condition

(i) $trN|_{E_{2*}} = 0$, (ii) $\det N|_{E_{2*}} > 0$ and
(ii) $\frac{d}{d\rho}trN|_{E_{2*}} = -1 \neq 0$ at $\rho = \rho^{[hf]}$.

This guarantees the existence of Hopf-bifurcation around $E_{2*}(u_{2*}, u_{2*})$. The stability of limit cycle is discussed in section "Case-I: $h > c$".

Remark 2 From the above Theorem it is clear that if $(2+b)\bar{u}^2 + (\rho+c-1)\bar{u} + \rho c > 0$, then one of the eigenvalue of Jacobian matrix at the saddle-node equilibrium point $\bar{E}(\bar{u}, \bar{u})$ is negative and the other is zero. This shows that $\bar{E}(\bar{u}, \bar{u})$ is a non-hyperbolic equilibrium point so there is a chance of bifurcation around the saddle-node equilibrium point $\bar{E}(\bar{u}, \bar{u})$.

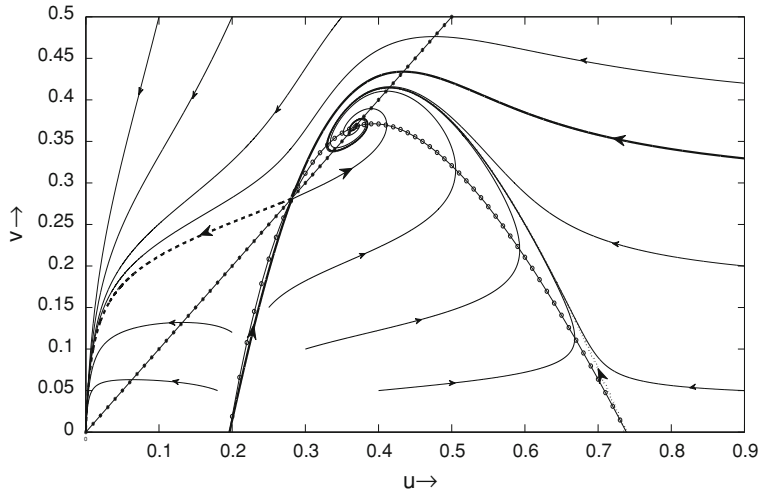

Fig. 2 Here *star marked line* is predator nullcline and *circle marked curve* is prey nullcline. *Light dotted curves* are stable manifolds for E_{2*} and unstable manifolds for E_H while *dashed curve* is stable manifolds for $(0, 0)$ and unstable manifold for E_{1*}. *Dark solid curve* is a seperatrix which divides the whole region into two parts.

Numerical Examples

In order to verify the above results we shall consider following numerical examples by taking the numerical data $b = 0.400$, $c = 0.065$, $h = 0.210$ which gives $\rho^{[hf]} = 0.0459$ then

(i) For $\rho = 0.100 > \rho^{[hf]}$ together with above data, the two interior equilibrium points $E_{1*} = (0.282, 0.282)$ and $E_{2*} = (0.367, 0.367)$ are shown in Fig. 2 where E_{1*} is saddle point and E_{2*} is stable focus. In this case there is a seperatrix which divides the region $Int(\Omega)$ into two parts. Trajectories initiating from one side of the seperatrix approach to the interior equilibrium point E_{2*} and trajectories initiating from other side of seperatrix approach to the origin $(0, 0)$. Therefore we can say that the region from one side of the seperatrix is the omega limit set of the interior equilibrium point E_{2*} and the region from other side of seperatrix omega limit set of $(0, 0)$.

(ii) For $\rho = \rho^{[hf]}$, the two interior equilibrium points are shown in Fig. 3, where $E_{1*} = (0.282, 0.282)$ is a saddle point and an unstable limit cycle appears through Hopf bifurcation in a small neighborhood of $E_{2*} = (0.367, 0.367)$.

(iii) For $\rho = 0.040 < \rho^{[hf]}$, Fig. 4 shows the two interior equilibria are $E_{1*} = (0.282, 0.282)$ is a saddle point and $E_{2*} = (0.367, 0.367)$ is an unstable focus. In this case all the solutions of system (5) converge to the origin, biologically we say that for all initial value the system goes to extinction.

From above three examples it is clear that the position of equilibrium points does not change in the three cases as the expression for equilibrium points is independent of ρ but the stability of the equilibrium point $E_{2*} = (0.367, 0.367)$ changes and it becomes unstable to stable as ρ passes though $\rho^{[hf]}$ from right to left.

For $b = 0.400, c = 0.065, h = h^{[sn]} = 0.212$ and $\rho = 0.250$, Fig. 5 shows that the saddle-node equilibrium point $\bar{E} = (0.325, 0.325)$ is non-hyperbolic saddle point. In this case also there is a seperatrix which divides the region $Int(\Omega)$ into two parts. Trajectories

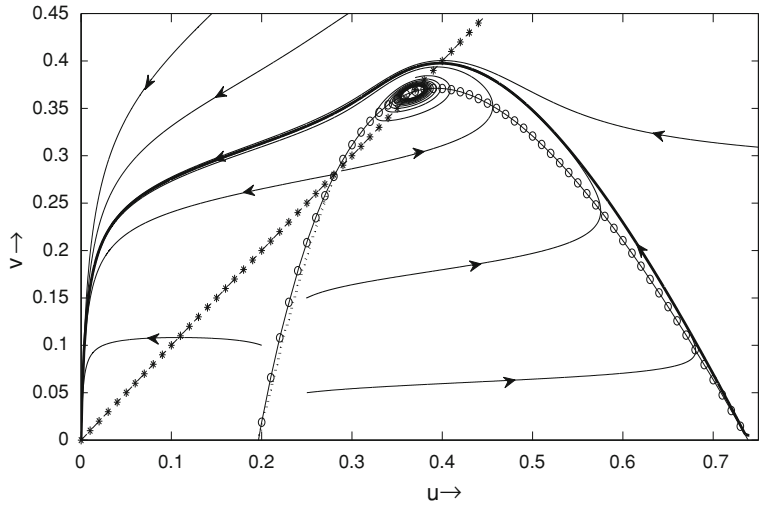

Fig. 3 The interior equilibrium point $E_{1*} = (0.282, 0.282)$ is a saddle point and an unstable limit cycle around $E_{2*} = (0.367, 0.367)$. Here also *star marked line* is predator nullcline and *circle marked curve* is prey nullcline. *Dark solid curve* is unstable manifold for E_H and stable manifold for $(0, 0)$. *Dotted curve* is stable manifold for E_{1*} and unstable manifold for E_L.

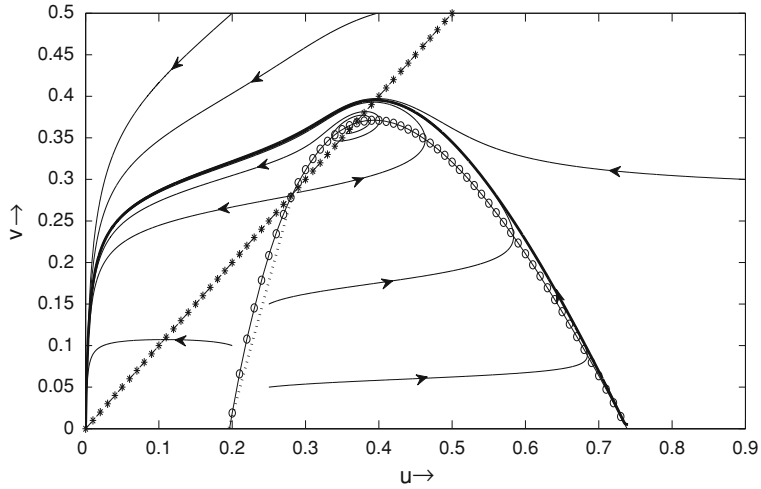

Fig. 4 Two interior equilibrium points with $E_{1*} = (0.282, 0.282)$ a saddle point and $E_{2*} = (0.367, 0.367)$ an unstable focus. Here also *star marked line* is predator nullcline and *circle marked curve* is prey nullcline. *Dotted curve* is stable manifold for E_{1*} and unstable manifold for E_H. *Dark solid curve* is unstable manifold for E_H and stable manifold for $(0, 0)$

initiating from one side of the seperatrix approach to the interior equilibrium point $\bar{E}$ and trajectories initiating from other side of seperatrix approach to $(0, 0)$. The region from one side of the seperatrix is the omega limit set of the interior equilibrium point $\bar{E}$ and the region from other side of seperatrix omega limit set of $(0, 0)$.

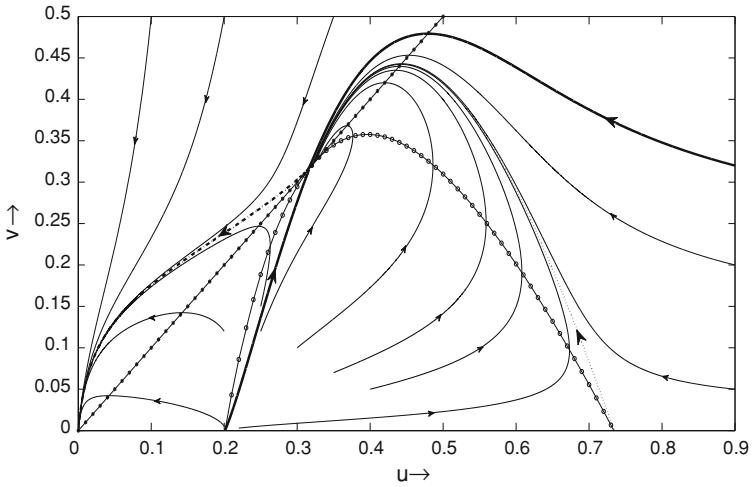

Fig. 5 The saddle-node equilibrium point $\bar{E} = (0.325, 0.325)$ is non-hyperbolic saddle point. Here *dotted curve* is stable manifolds for $\bar{E}$ and unstable manifolds for axial equilibrium E_H while *dark dash-dotted curve* is stable manifolds for $(0, 0)$. *Dark solid curve* is a seperatrix which divides the whole region into two parts. Trajectories initiating from one side of the seperatrix approach to the interior equilibrium point $\bar{E}$ tangential to the stable manifold (*dotted curve*) of $\bar{E}$ and trajectories initiating from other side of seperatrix approach to $(0, 0)$ tangential to the stable manifold (*dark dash-dotted curve*) of $(0, 0)$.

From the above three diagrams it is clear that the stability of the interior equilibrium point $E_{2*} = (0.367, 0.367)$ changes and it becomes unstable to stable as ρ passes though $\rho^{[hf]}$ from right to left.

Saddle-Node Bifurcation

Theorem 3 *The system (5) undergoes a saddle-node bifurcation around $\bar{E}(\bar{u}, \bar{u})$ with respect to bifurcation parameter h if $(1 - c(b + 1))^2 = 4(b + 1)(h - c)$ and $(2 + b)\bar{u}^2 + (\rho + c - 1)\bar{u} + \rho c > 0$.*

Proof To prove that the model (5) undergoes a saddle-node bifurcation, we use Sotomayor's theorem [9,18] by considering h as the bifurcation parameter.
In order to apply Sotomayor's theorem one of the eigenvalue of the Jacobian at the saddle-node equilibrium point must be zero and the other eigenvalue must have negative real part, so we need to take the condition $(2 + b)\bar{u}^2 + (\rho + c - 1)\bar{u} + \rho c > 0$. Let $g = (g^{(1)}, g^{(2)})^T$ with $g^{(1)} \equiv uf^{(1)}$ and $g^{(2)} \equiv vf^{(2)}$ where $f^{(1)}$ and $f^{(2)}$ are already defined in section "Mathematical Model".

The Jacobian $\overline{J}$ at the equilibrium point $\bar{E}(\bar{u}, \bar{u})$ is given by

$$\overline{J} \equiv Dg(\bar{u}, \bar{u}) = \begin{pmatrix} \xi_1 & \xi_2 \\ \omega_1 & \omega_2 \end{pmatrix},$$

where $\xi_1 = 1 - (2 + b)\bar{u} - \frac{hc}{(c+\bar{u})^2}$, $\xi_2 = -b\bar{u}$, $\omega_1 = \rho$ and $\omega_2 = -\rho = -\omega_1$.
Let $h^{[sn]}$ be the value of h such that the matrix $\overline{J}$ has a simple zero eigenvalue at $h = h^{[sn]}$. This demands $\det \overline{J} \mid_{h=h^{[sn]}} = \xi_1\omega_2 - \xi_2\omega_1 \mid_{h=h^{[sn]}} = 0$, this requires $\xi_1 + \xi_2 = 0$.
Since $tr\overline{J} < 0$, if $(2 + b)\bar{u}^2 + (\rho + c - 1)\bar{u} + \rho c > 0$ so one of the eigenvalue of $\overline{J}$ at

$h = h^{[sn]}$ is negative.

Now, let $V = (v_1, v_2)^T$ and $W = (w_1, w_2)^T$ be the eigenvectors of $\overline{J}$ and $\overline{J}^T$ corresponding to zero eigenvalue respectively, a simple calculation yields $V = (1, 1)^T$ and $W = (1, \frac{\xi_2}{\omega_1})^T$. Therefore, $\Omega_1 = W^T.g_h(\bar{E}, h^{[sn]}) = -\frac{\bar{u}}{c+\bar{u}} < 0$ at $h = h^{[sn]}$, since

$$g_h(\bar{E}, h^{[sn]}) \equiv \frac{\partial g}{\partial h}(\bar{E}, h^{[sn]}) = \begin{pmatrix} -\frac{\bar{u}}{c+\bar{u}} \\ 0 \end{pmatrix} \text{ at } h = h^{[sn]}.$$

Now, $\Omega_2 = W^T[D^2 g(\bar{E}, h^{[sn]})(V, V)]$, where

$$D^2 g\left(X = (u, v)^T, h\right) = \begin{pmatrix} \nabla \frac{\partial g^{(1)}}{\partial u} & \nabla \frac{\partial g^{(1)}}{\partial v} \\ \nabla \frac{\partial g^{(2)}}{\partial u} & \nabla \frac{\partial g^{(2)}}{\partial v} \end{pmatrix},$$

$$\nabla \frac{\partial g^{(i)}}{\partial u} = \left(\frac{\partial^2 g^{(i)}}{\partial u^2}, \frac{\partial^2 g^{(i)}}{\partial u \partial v} \right)^T \text{ and } \nabla \frac{\partial g^{(i)}}{\partial v} = \left(\frac{\partial^2 g^{(i)}}{\partial u \partial v}, \frac{\partial^2 g^{(i)}}{\partial u^2} \right)^T \text{ for } i = 1, 2.$$

Therefore,

$$\Omega_2 = \begin{pmatrix} 1 & \frac{\xi_2}{\omega_1} \end{pmatrix} \begin{pmatrix} g_{uu}^{(1)} v_1^2 + 2 g_{uv}^{(1)} v_1 v_2 + g_{vv}^{(1)} v_2^2 \\ g_{uu}^{(2)} v_1^2 + 2 g_{uv}^{(2)} v_1 v_2 + g_{vv}^{(2)} v_2^2 \end{pmatrix} \text{at } h = h^{[sn]}.$$

i.e., $\Omega_2 = \begin{pmatrix} 1 & \frac{\xi_2}{\omega_1} \end{pmatrix} \begin{pmatrix} -2 + \frac{2hc}{(c+\bar{u})^3} - 2b \\ 0 \end{pmatrix}$ at $h = h^{[sn]}$. Hence $\Omega_2 = -2(b+1) + \frac{2hc}{(c+\bar{u})^3}$. Now using $\xi_1 + \xi_2 = 0$ and $\bar{u} = \frac{1-c(b+1)}{2(b+1)}$, we have $\frac{hc}{(c+\bar{u})^2} = c(b+1)$, so $\Omega_2 = -\frac{2(b+1)}{c(b+1)+1}(1 - c(b+1)) < 0$ as $(1 - c(b+1)) > 0$. Thus from Sotomayor's theorem the system undergoes a saddle-node bifurcation around $\bar{E}(\bar{u}, \bar{u})$ at $h = h^{[sn]}$. Hence, we conclude that when the parameter h passes from one side of $h = h^{[sn]}$ to the other side, the number of interior equilibria of system (5) changes from zero to two (see Fig. 6).

The biological interpretation for the saddle-node bifurcation is that $h_{MSY} = h^{[sn]}$. Both the species are driven to extinction, and the system collapses for $h > h^{[sn]}$. But the species do not go to extinction for a wide range of initial data when $0 < h < h^{[sn]}$, i.e., coexistence for model (5) is possible in the form of a positive equilibrium for certain choices of initial values.

Stability of Limit Cycle

In order to discuss the stability (direction) of limit cycle we now compute the Lyapunov coefficient σ [18] at the point $E_{2*}(u_{2*}, u_{2*})$ of the system (5).

We first translate the equilibrium $E_{2*}(u_{2*}, u_{2*})$ of system (5) to the origin by using the transformation $u = \hat{u} - u_{2*}$ and $v = \hat{v} - u_{2*}$. Then, system (5) in a neighborhood of the origin can be written as

$$\begin{cases} \frac{d\hat{u}}{d\tau} = -\frac{hu_{2*}}{c+u_{2*}} + u_{2*} - bu_{2*}\hat{v} - {u_{2*}}^2 - bu_{2*}{}^2 + \left(-2u_{2*} - b\hat{v} + \frac{hu_{2*}}{(c+u_{2*})^2} - bu_{2*} - \frac{h}{c+u_{2*}} + 1 \right)\hat{u} \\ \quad + \left(-1 - \frac{hu_{2*}}{(c+u_{2*})^3} + \frac{h}{(c+u_{2*})^2} \right)\hat{u}^2 + \left(\frac{hu_{2*}}{(c+u_{2*})^4} - \frac{h}{(c+u_{2*})^3} \right)\hat{u}^3 + F_1(\hat{u}, \hat{v}), \\ \frac{d\hat{v}}{d\tau} = \frac{\rho\hat{u}^3}{{u_{2*}}^2} - \frac{\rho\hat{u}^2}{u_{2*}} + \rho\hat{u} + \left(-\rho + 2\frac{\rho\hat{u}^3}{{u_{2*}}^3} - 2\frac{\rho\hat{u}^2}{{u_{2*}}^2} + 2\frac{\rho\hat{u}}{u_{2*}} \right)\hat{v} + \left(\frac{\rho\hat{u}}{{u_{2*}}^2} - \frac{\rho}{u_{2*}} + \frac{\rho\hat{u}^3}{{u_{2*}}^4} - \frac{\rho\hat{u}^2}{{u_{2*}}^3} \right)\hat{v}^2 + F_2(\hat{u}, \hat{v}), \end{cases} \tag{14}$$

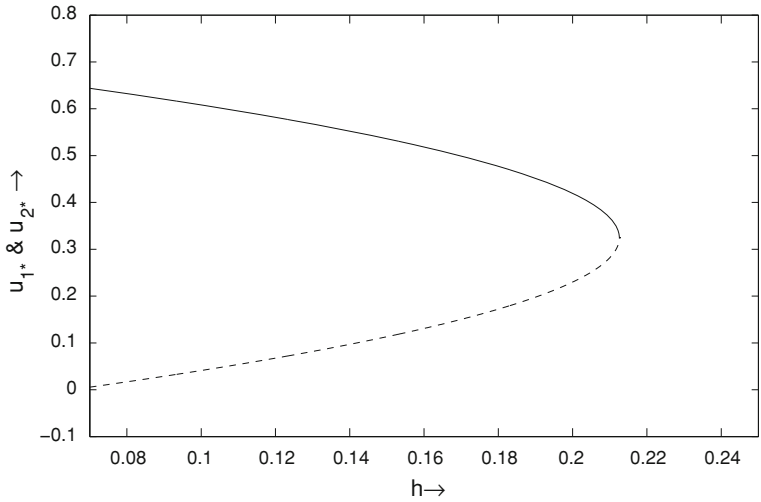

Fig. 6 Bifurcation of interior equilibria with respect to h. Here *solid curve* stands for first component of stable equilibrium point $E_{2*}(u_{2*}, u_{2*})$ and *dashed curve* shows first component of unstable equilibrium point $E_{1*}(u_{1*}, u_{1*})$.

where $F_k(\hat{u}, \hat{v})$ (for $k = 1, 2$) are power series in powers of $\hat{u}^i \hat{v}^j$ satisfying $i + j \geq 4$.

Now using equilibrium Eq. (11) system (14) can be rewritten as

$$\begin{cases} \frac{d\hat{u}}{d\tau} = a_{10}\hat{u} + a_{01}\hat{v} + a_{20}\hat{u}^2 + a_{11}\hat{u}\hat{v} + a_{02}\hat{v}^2 + a_{30}\hat{u}^3 + a_{21}\hat{u}^2\hat{v} + a_{12}\hat{u}\hat{v}^2 + a_{03}\hat{v}^3 + F_1(\hat{u}, \hat{v}), \\ \frac{d\hat{v}}{d\tau} = b_{10}\hat{u} + b_{01}\hat{v} + b_{20}\hat{u}^2 + b_{11}\hat{u}\hat{v} + b_{02}\hat{v}^2 + b_{30}\hat{u}^3 + b_{21}\hat{u}^2\hat{v} + b_{12}\hat{u}\hat{v}^2 + b_{03}\hat{v}^3 + F_2(\hat{u}, \hat{v}), \end{cases} \tag{15}$$

where $a_{10} = 1 - 2u_{2*} - bu_{2*} - \frac{hc}{(c+u_{2*})^2}$, $a_{01} = -bu_{2*}$, $a_{20} = -1 - \frac{hu_{2*}}{(c+u_{2*})^3} + \frac{h}{(c+u_{2*})^2}$, $a_{11} = -b$, $a_{02} = 0$, $a_{30} = \frac{hu_{2*}}{(c+u_{2*})^4} - \frac{h}{(c+u_{2*})^3}$, $a_{21} = 0$, $a_{12} = 0$, $a_{03} = 0$, $b_{10} = \rho$, $b_{01} = -\rho$, $b_{20} = -\frac{\rho}{u_{2*}}$, $b_{11} = \frac{2\rho}{u_{2*}}$, $b_{02} = -\frac{\rho}{u_{2*}}$, $b_{30} = \frac{\rho}{{u_{2*}}^2}$, $b_{21} = \frac{2\rho}{{u_{2*}}^2}$, $b_{12} = \frac{\rho}{{u_{2*}}^2}$, $b_{03} = 0$

with $F_1(\hat{u}, \hat{v}) = \Sigma_{i+j=4}^{\infty} a_{ij}\hat{u}^i\hat{v}^j$ and $F_2(\hat{u}, \hat{v}) = \Sigma_{i+j=4}^{\infty} b_{ij}\hat{u}^i\hat{v}^j$

Hence the first Lyapunov coefficient σ for planar system (as defined in [18]) is given by

$$\begin{aligned} \sigma = -\frac{3\pi}{2a_{02}\Delta^{3/2}}\{&[a_{10}b_{10}(a_{11}{}^2 + a_{11}b_{02} + a_{02}b_{11}) + a_{10}a_{01}(b_{11}{}^2 + a_{20}b_{11} + a_{11}b_{02}) \\ &+b_{10}{}^2(a_{11}a_{02} + 2a_{02}b_{02}) - 2a_{10}b_{10}(b_{02}{}^2 - a_{20}a_{02}) - 2a_{10}a_{01}(a_{20}{}^2 - b_{20}b_{02}) \\ &-a_{01}{}^2(2a_{20}b_{20} + b_{11}b_{20}) + (a_{01}b_{10} - 2a_{10}{}^2)(b_{11}b_{02} - a_{11}a_{20})] \\ &-(a_{10}{}^2 + a_{01}b_{10})[3(b_{10}b_{03} - a_{01}a_{30}) + 2a_{10}(a_{21} + b_{12}) + (b_{10}a_{12} - a_{01}b_{21})]\}, \end{aligned}$$

where $\Delta = \frac{\rho u_{2*}}{c+u_{2*}}\sqrt{(1 - c(b+1))^2 - 4(b+1)(h-c)}$.

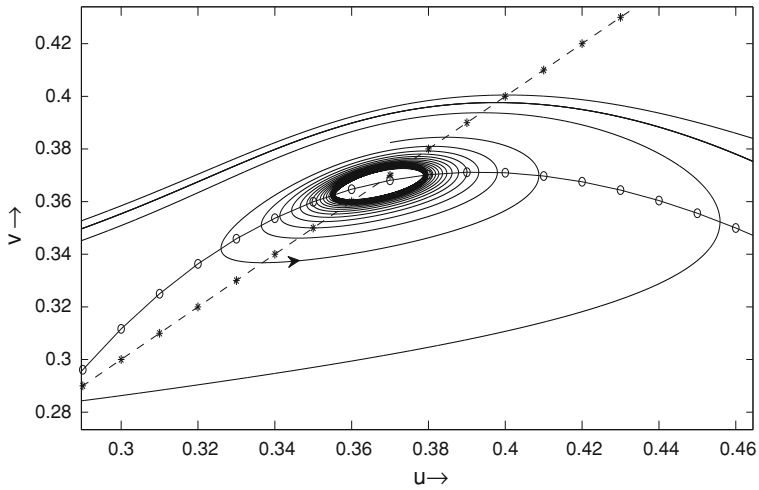

Fig. 7 This figure is zoomed version of the Fig. 3 which shows that the limit cycle around the equilibrium point $E_{2*}(u_{2*}, u_{2*}) = (0.367, 0.367)$ is unstable.

After a tedious computation using MAPLE we get

$$\sigma = -\frac{3\pi}{2\Delta^{3/2} b {u_{2*}}^3} Q,$$

where $Q = 3b\,\rho^2 u_{2*}\,a_{10} + 2b\,\rho {u_{2*}}^2\,a_{10}a_{20} + 2\,\rho^3\,a_{10} - 2\,b{u_{2*}}^3\,a_{10}{a_{20}}^2 - b^2\rho {u_{2*}}^3 a_{20}$

$-2\,b\rho^3 u_{2*} - 4\rho^2\,{a_{10}}^2 + 2b\,{u_{2*}}^2\,{a_{10}}^2 a_{20} + 3b{u_{2*}}^3\,{a_{10}}^2 a_{30} + 2\rho\,{a_{10}}^3 - 2bu_{2*}\rho\,{a_{10}}^2 - 3\,b^2\rho\,{u_{2*}}^4\,a_{30}$.

Since the expression for Lyapunov number σ is complex enough so we can not say anything about the sign of σ and therefore we have given the following numerical example. For $b = 0.400, c = 0.065, h = 0.210 < h^{[sn]}$ the two interior equilibrium are given by $E_{1*}(u_{1*}, u_{1*}) = (0.282, 0.282)$ a saddle point and $E_{2*}(u_{2*}, u_{2*}) = (0.367, 0.367)$. For $\rho = \rho^{[hf]} = 0.045$ an unstable limit cycle appears through Hopf bifurcation in a small neighborhood of $E_{2*}(u_{2*}, u_{2*})$ as the Lyapunov number $\sigma = 309.6884832\pi > 0$ (see Fig. 7). Therefore an unstable limit cycle is created around the equilibrium point $E_{2*}(u_{2*}, u_{2*})$.

Case-II: $h < c$

Axial Equilibria

In this case $u = u_H$ is the only positive real root of Eq. (8). Since for $h < c$ the product of roots is negative therefore both the roots are either of opposite sign or complex conjugates. Hence the unique axial equilibrium point is

$$E_H = (u_H, 0) \equiv \left(\frac{1 - c + \sqrt{(1-c)^2 - 4(h-c)}}{2}, 0 \right),$$

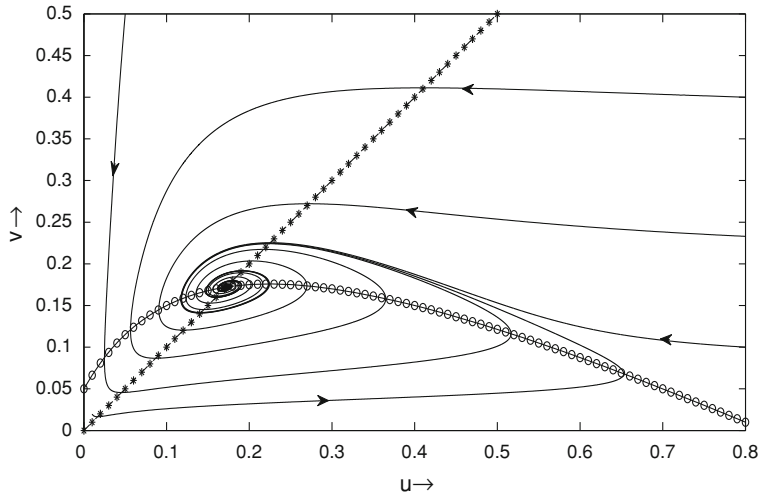

Fig. 8 The unique interior equilibrium $E_*(u_*, u_*) = (0.172, 0.172)$ is stable and axial equilibrium point is a saddle point.

Interior Equilibria

In this case u_{2*} given by (13), is the only positive real root of the Eq. (9), hence $E_{2*}(u_{2*}, u_{2*}) \equiv E_*(u_*, u_*)$ is the unique interior equilibrium point.

Stability and Hopf Bifurcation

Here we state the stability of equilibrium points and related bifurcation results only without any proof. The results can be proved in a similar manner as discussed in the previous section.

Theorem 4 *(a) The unique axial equilibrium point $E_H = (u_H, 0)$ is always a saddle point.*

(b) The unique interior equilibrium point $E_*(u_*, u_*)$ is stable if $(2 + b){u_*}^2 + (\rho + c - 1)u_* + \rho c > 0$.

(c) System (5) undergoes a Hopf bifurcation with respect to bifurcation parameter ρ around the equilibrium point $E_*(u_*, u_*)$ if $(2 + b){u_*}^2 + (\rho + c - 1)u_* + \rho c = 0$, i.e. a limit cycle is created around the unique interior equilibrium point $E_*(u_*, u_*)$ for certain value of ρ.

Numerical Examples

For $b = 2.000, c = 0.200, h = 0.180$ and $\rho = 0.2 > 0.052 = \rho^{[hf_1]}$, together with above parameter values, Fig. 8 shows that the unique interior equilibrium $E_*(u_*, u_*) = (0.172, 0.172)$ is stable on the other hand for $\rho = \rho^{[hf_1]} = 0.052$, together with above parameter values, Fig. 9 shows that a stable limit cycle appears through Hopf bifurcation around $E_*(u_*, u_*) = (0.172, 0.172)$ as the Lyapunov number $\sigma = -67.32782765\pi < 0$.

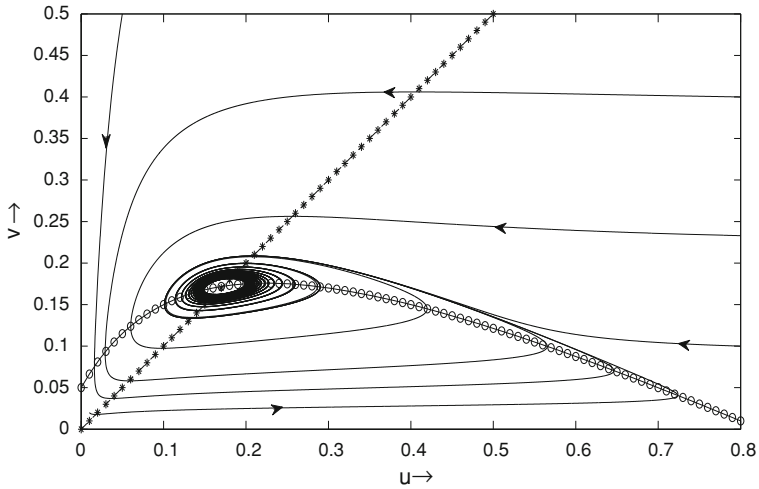

Fig. 9 A stable limit cycle around the unique interior equilibrium point $E_*(u_*, u_*) = (0.172, 0.172)$ and axial equilibrium point is a saddle point

Case-III: $h = c$

Axial Equilibria

The roots of Eq. (8) are zero and $u = 1 - c$ and hence $E_{10} = (1 - c, 0)$ is the only axial equilibrium point as $c < 1$.

Interior Equilibria

The roots of Eq. (9) are zero and $u = 1 - c(b + 1)$ and hence $E^*(u^*, u^*) = \left(\frac{1-c(b+1)}{b+1}, \frac{1-c(b+1)}{b+1}\right)$ is the only interior equilibrium point if $c(b + 1) < 1$.

Stability and Hopf Bifurcation

Theorem 5 *(a) The axial equilibrium point $E_{10} = (1 - c, 0)$ is always a saddle point.*

(b) The unique interior equilibrium point $E^*(u^*, u^*)$ is stable if $\left(c(b + 1)^2 - 1\right) u^* < \rho$.

(c) System (5) undergoes a Hopf bifurcation with respect to bifurcation parameter ρ around the equilibrium point $E^*(u^*, u^*)$ if $\left(c(b + 1)^2 - 1\right) u^* = \rho$, i.e. a limit cycle is created around the unique interior equilibrium point $E^*(u^*, u^*)$ for certain value of ρ.

The above result can be obtained in the same manner as discussed in section "Stability of Equilibria".

Numerical Examples

To verify the above result numerically we consider the following example:

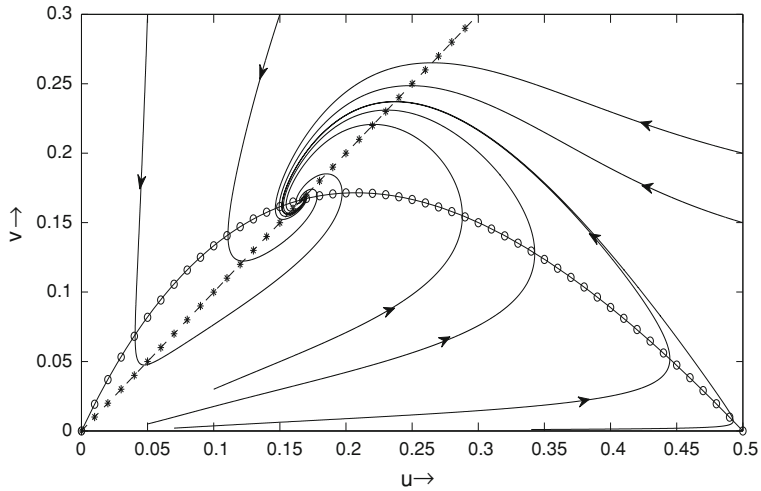

Fig. 10 For $b = 0.500$, $c = 0.500$, $h = 0.500$ and $\rho = 0.100 > \rho^{[hf_2]} = 0.020$, a unique stable interior equilibrium point is $E^* = (0.167, 0.167)$

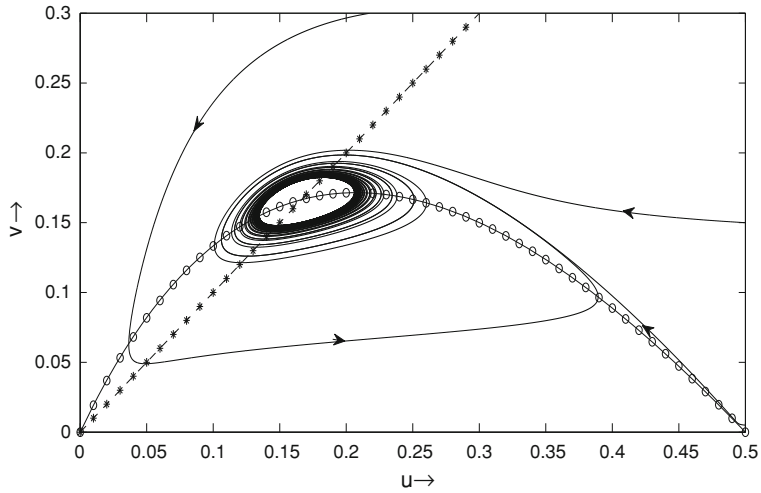

Fig. 11 For $b = 0.500$, $c = 0.500$, $h = 0.500$ and $\rho = \rho^{[hf_2]} = 0.020$, a stable limit cycle is created around the unique interior equilibrium point $E^* = (0.167, 0.167)$. Amplitude of limit cycle increase as ρ decreases from $\rho = 0.020$

For $b = 0.500$, $c = 0.500$, $h = 0.500$, Fig. 10 shows that the unique interior equilibrium point $E^*(u^*, u^*) = (0.167, 0.167)$ is stable for $\rho = 0.100 > \rho^{[hf_2]} = 0.020$. On the other hand for $\rho = \rho^{[hf_2]} = 0.020$, Fig. 11 shows that a stable limit cycle appears through Hopf bifurcation around $E_*(u_*, u_*)$ as the Lyapunov number $\sigma = -114.6086008\pi < 0$.

Asymptotic Behavior of the System (5) at (0, 0)

At the equilibrium point $E_0 = (0, 0)$, the Jacobian matrix cannot be calculated directly because the ratio $\frac{v}{u}$ is not defined at this point. To understand the stability behavior of this

point we must expand it on whole axis by studying the transformed system induced from the transformation $u = \phi,\ v = \phi\psi$ [11].

Theorem 6 *The equilibrium point $E_0 = (0, 0)$ of the system (5) is an attractor point if $h > c$ and a saddle point for $h < c$.*

Proof Consider the transformation $u = \phi,\ v = \phi\psi$, then we have

$$\frac{d\phi}{d\tau} = \frac{du}{d\tau} \quad \text{and} \quad \frac{d\psi}{d\tau} = \frac{1}{\phi}\left(\frac{dv}{d\tau} - \psi\frac{d\phi}{d\tau}\right)$$

Under this transformation (5) transformed to the following system

$$\begin{cases} \frac{d\phi}{d\tau} = \phi\left(1 - \phi - b\phi\psi - \frac{h}{c+\phi}\right), \\ \frac{d\psi}{d\tau} = \psi\left(\rho(1-\psi) - 1 + \phi + b\phi + \frac{h}{c+\phi}\right). \end{cases} \tag{16}$$

There are two equilibria on the ψ-axis, $(0, 0)$ and $\left(0, \frac{\rho c+h-c}{\rho c}\right)$ if $\rho c + h > c$.
The Jacobian matrix for the system (16) at $(0, 0)$ is given by

$$Q = \begin{pmatrix} \frac{c-h}{c} & 0 \\ 0 & \frac{\rho c+h-c}{c} \end{pmatrix}.$$

Therefore $(0, 0)$ is a hyperbolic saddle point for the system (16) if $h > c$ and is unstable if $h < c$ under the existence of the singularity $\left(0, \frac{\rho c+h-c}{\rho c}\right)$.
Now the Jacobian matrix for the system (16) at $\left(0, \frac{\rho c+h-c}{\rho c}\right)$ is given by

$$R = \begin{pmatrix} \left(\frac{\rho c+h-c}{\rho c}\right)\left(1 + b - \frac{h}{c^2}\right) & \frac{c-h}{c} \\ -\rho\left(\frac{\rho c+h-c}{\rho c}\right) & 0 \end{pmatrix}.$$

From the above matrix it is clear that the equilibrium point $\left(0, \frac{\rho c+h-c}{\rho c}\right)$, for the system (16) is an attractor point if $h > c$ (see Fig. 12) and a saddle point if $h < c$ (see Fig. 8). Therefore the point $(0, 0)$ is then an attractor point if $h > c$ and a saddle point if $h < c$, for the system (5).

Remark 3 System (5) has no interior equilibrium point and $E_0 = (0, 0)$ is a global attractor if $(i)\ h = c$ and $(ii)\ c(b + 1) = 1$. In this case, the topological structure of the origin in $Int(\Omega)$ consists of an elliptic sector and a parabolic sector (see Fig. 13).

In the next section, we discuss the existence conditions for the bionomic equilibrium point for the model (3) which is the combination of biological and economic equilibrium point.

Bionomic Equilibria

The bionomic equilibrium is said to be achieved when the total revenue obtained by selling the harvested biomass equals the total cost utilized in harvesting it. The economic interest of the yield of the harvest effort is the Net Economic Revenue which is given by:

Net Economic Revenue (N.E.R.) = Total Revenue (T.R.) – Total Cost (T.C.),

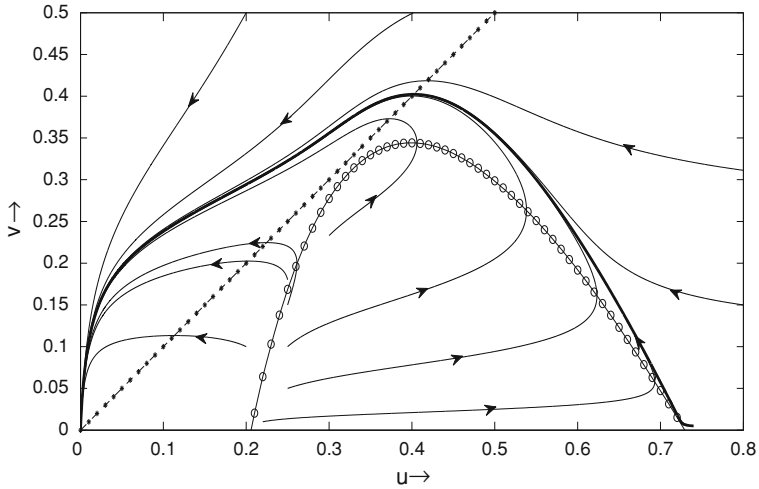

Fig. 12 For $b = 0.400, c = 0.065, h = 0.215$ and $\rho = 0.1$, no interior equilibrium point and in this case system goes to extinction and $(0, 0)$ is an attractor

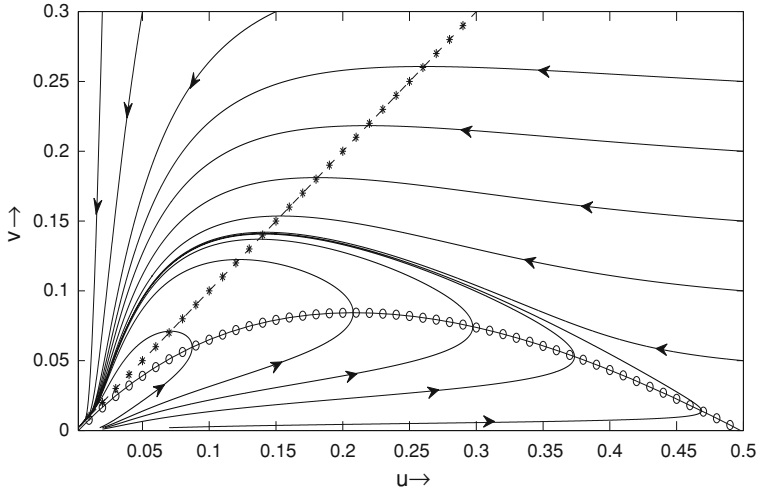

Fig. 13 For $b = 1.000, h = c = 0.500$ and $\rho = 0.050$, the equilibrium point $(0, 0)$ of system (5) is a global attractor and $(1 - c, 0)$ is a saddle point

where $T.R. = pqEx/(m_1E + m_2x)$ and $T.C. = CE$ with C being the constant harvesting cost per unit effort and p being the constant price per unit biomass of prey species.
Thus the net profit at any time [5] is given by

$$P(x, E) = \left(\frac{pqx}{m_1E + m_2x} - C\right)E, \tag{17}$$

Note that if the harvesting cost is greater than the revenue for prey species (i.e. $C > \frac{pqx}{m_1E+m_2x}$), then harvesting in prey species is not profitable and so it is not of interest. Hence

to continue the harvesting we consider here the cost must be less than the revenue for prey species (i.e. $C < \frac{pqx}{m_1E+m_2x}$).

The bionomic equilibrium $(x_\infty, y_\infty, E_\infty)$ is given by the positive solutions of $\frac{dx}{dt} = \frac{dy}{dt} = P = 0$, i.e.,

$$r\left(1-\frac{x}{K}\right) - \alpha y - \frac{qE}{m_1E+m_2x} = 0, \tag{18}$$

$$y = nx, \tag{19}$$

$$\frac{pqx}{m_1E+m_2x} - C = 0. \tag{20}$$

Hence one can say that the bionomic equilibria is the point of intersection of biological equilibrium line and zero profit line. From Eqs. (15), (19) and (20) we get the bionomic equilibrium as follows

$$x_\infty = \frac{K(Cm_2 + rm_1p - pq)}{m_1p(r+\alpha nK)}, \quad y_\infty = nx_\infty \quad \text{and} \quad E_\infty = \frac{pq - Cm_2}{Cm_1}x_\infty$$

if $\frac{Cm_2}{p} < q < \frac{Cm_2}{p} + rm_1$.

Singular Optimal Control

In this section, our objective is to maximize the current value of continuous time stream of revenues which is given by

$$J(x, E) = \int_0^\infty e^{-\delta t} P(x, E)dt, \tag{21}$$

where δ denotes the continuous annual discount rate which is fixed by harvesting agencies. We shall maximize (21) together with the steady state Eqs. (18) and (19) with the help of Pontryagin's Maximum Principle [19]. The control variable E is subjected to the constraint $0 \le E \le E_{max}$, where E_{max} is a feasible upper limit for the harvesting effort.
Therefore, the optimal control problems over an infinite time horizon is given by

$$\max_{0\le E(t)\le E_{max}} \int_0^\infty e^{-\delta t} P(x, E)dt, \tag{22}$$

subject to the Eqs. (3) with $(x, y) \neq (0, 0)$ and $x(0) = x_0,\ y(0) = y_0$.

In order to find an optimal equilibrium (i. e. the interior equilibrium corresponding to the optimal effort) it is necessary that the optimal equilibrium point must be at least locally asymptotically stable, so that the optimal path would consist of a path which leads to the optimal equilibrium level as quickly as possible and then stays there with that optimal effort subsequently [13]. This can be ensured if the parameters (b, c, h, ρ) lie in the region $S = S_1 \cup S_2 \cup S_3$, where

$$\begin{aligned} S_1 = \{&(b, c, h, \rho) \in R_+^4 \mid h > c,\ c(b+1) < 1,\ (1-c(b+1))^2 - 4(b+1)(h-c) > 0,\\ &(2+b){u_{2*}}^2 + (\rho + c - 1)u_{2*} + \rho c > 0\},\\ S_2 = \{&(b, c, h, \rho) \in R_+^4 \mid h < c,\ (2+b){u_{2*}}^2 + (\rho + c - 1)u_{2*} + \rho c > 0\} \end{aligned}$$

and

$$S_3 = \{(b, c, h, \rho) \in R_+^4 \mid h = c,\ c(b+1) < 1,\ \left(c(b+1)^2 - 1\right) u^* < \rho\}.$$

The associated Hamiltonian function is given by

$$H(x, y, E, t) = \left(\frac{pq\,x}{m_1 E + m_2 x} - C\right) E e^{-\delta t} + \lambda_1 \left(r\left(1 - \frac{x}{K}\right) - \alpha y - \frac{q\,E}{m_1 E + m_2 x}\right) x + \lambda_2 s \left(1 - \frac{y}{n\,x}\right) y,$$

where $\lambda_i = \lambda_i(t),\ i = 1, 2$ are adjoint variables.
Differentiating the Hamiltonian H with respect to the control variable E, we get

$$\frac{\partial H}{\partial E} = \left(\frac{pqm_2x^2}{(m_1E + m_2x)^2} - C\right) e^{-\delta t} - \lambda_1 \frac{qm_2x^2}{(m_1E + m_2x)^2} \tag{23}$$

The considered control problem admits a singular solution on the control set $[0, E_{max}]$, if $\frac{\partial H}{\partial E} = 0$, which gives

$$\lambda_1 e^{\delta t} = p - \frac{C(m_1E + m_2x)^2}{qm_2x^2}, \tag{24}$$

where $\lambda_1 e^{\delta t}$ is the usual shadow price [6].

In order to find the path of a singular control, Pontryagin's Maximum Principle [19] is utilized and the adjoint variables must satisfy the adjoint equations given by

$$\frac{d\lambda_1}{dt} = -\frac{\partial H}{\partial x} \quad \text{and} \quad \frac{d\lambda_2}{dt} = -\frac{\partial H}{\partial y}. \tag{25}$$

Since, we are looking for singular optimal equilibrium solution, so we use steady state Eqs. (15) and (19) in terms of x^* and $y^* = nx^*$, hence x^*, y^* and E can be taken as constant [12]. Thus Eq. (25) along with steady steady state Eqs. (18) and (19) give

$$\frac{d\lambda_1}{dt} = \lambda_1 \left(\frac{x^*}{K} - \frac{qm_2E\,x^*}{(m_1E + m_2x^*)^2}\right) - \lambda_2 n\,s - \frac{pqm_1E^2}{(m_1E + m_2x^*)^2} e^{-\delta t}, \tag{26}$$

$$\frac{d\lambda_2}{dt} = s\lambda_2 + \lambda_1 \alpha x^*. \tag{27}$$

Due to the presence of the term $e^{-\delta t}$ no steady state is possible for the above system. Hence we consider the following transformation [21].

$$\lambda_i(t) = \mu_i(t) e^{-\delta t}, \quad i = 1, 2,$$

where μ_i represents the present value of the adjoint variable λ_i.
Using Eq. (24), the Eq. (27) can be written in terms of μ_2 as follows:

$$\frac{d\mu_2}{dt} - (s + \delta)\mu_2 = -P_1(x^*). \tag{28}$$

where $P_1(x^*) = \alpha x^* \left(\frac{C(m_1E + m_2x^*)^2}{qm_2x^{*2}} - p\right)$.

The shadow prices $\mu_i = \lambda_i(t) e^{\delta t}, i = 1, 2$ should remain constant over time in singular equilibrium to satisfy the transversality conditions at ∞ (i. e. $\lim_{t\to\infty} \lambda_i(t) = 0$, for $i =$

1, 2). Thus the solution of Eq. (28) satisfying the transversality condition for discounted autonomous infinite horizon problem (22) is given by

$$\mu_2(t) = \frac{P_1(x^*)}{s+\delta}.$$

Using the above value of μ_2 the Eq. (26) can be written in the terms of μ_1 as follows:

$$\frac{d\mu_1}{dt} - (Q_1(x^*) + \delta)\mu_1 = -Q_2(x^*), \tag{29}$$

where, $Q_1(x^*) = \frac{x^*}{K} - \frac{qm_2E\,x^*}{(m_1E+m_2x^*)^2}$ and $Q_2(x^*) = \frac{pqm_1E^2}{(m_1E+m_2x^*)^2} + \frac{n\,s\,P_1(x^*)}{s+\delta}$.

Solution of the Eq. (29) satisfying the transversality condition at ∞ is given by

$$\mu_1(t) = \frac{Q_2(x^*)}{Q_1(x^*)+\delta}. \tag{30}$$

From Eqs. (24) and (30) we get

$$\frac{pqm_2x^{*2}}{(m_1E+m_2x^*)^2} - C = \left(\frac{Q_2}{Q_1+\delta}\right)\frac{qm_2x^{*2}}{(m_1E+m_2x^*)^2}, \tag{31}$$

Equation (31) gives the desired singular path [4] which is shown in Fig. 14.
The Eq. (31) along with steady state Eqs. (18) and (19) reduce to the following cubic polynomial equation in x^*

$$f(x^*) \equiv A_1x^{*3} + A_2x^{*2} + A_3x^* + A_4 = 0, \tag{32}$$

where, A_1, A_2, A_3 and A_4 are found using MAPLE and are given in the "Appendix".

It may be pointed out that the coefficient A_1 is always positive, hence the Eq. (32) will have at least one positive real root for x^* if $A_4 < 0$. Equivalently, we can say that if

$$\begin{aligned} &pm_1{}^2r^3 + m_1\left(-\delta\, pm_1 + Cm_2 - 2\,pq\right)r^2 + q\left(pq + 2\,\delta\, pm_1 - Cm_2\right)r \\ &\quad + \delta\, q\left(-pq + Cm_2\right) > 0 \end{aligned}$$

then Eq. (32) will have at least one positive real root for x^* which together with steady state Eqs. (18) and (19) gives the singular equilibrium point

$$(x^*, y^*, E^*) = \left(x^*, nx^*, \frac{m_2x^*(rK - rx^* - \alpha nKx^*)}{rm_1x^* + \alpha nKm_1x^* + qK - rKm_1}\right).$$

Notice that

$$\frac{\partial^2 H(x^*, y^*, E^*, t)}{\partial x^2} = -\frac{2\lambda_1 r}{K} - \frac{2m_1E^{*2}}{x^{*2}(m_1E^* + m_2x^*)}\left(\frac{\partial H}{\partial E} + Ce^{-\delta t}\right) - \frac{2\lambda_2 sn}{x^*}$$

and

$$\frac{\partial^2 H(x^*, y^*, E^*, t)}{\partial y^2} = -\frac{2\lambda_2 s}{nx^*}.$$

Therefore in the case of singular control (i.e. $\frac{\partial H}{\partial E} = 0$)

$$\frac{\partial^2 H}{\partial x^2} < 0 \text{ and } \frac{\partial^2 H}{\partial y^2} < 0 \text{ for all } t \in [0, \infty)$$

provided $\lambda_i(t),\ i = 1, 2$ are positive i.e. $P_1(x^*) > 0$ and $Q_1(x^*) + \delta > 0$ which gives

$$\frac{C(m_1E + m_2x^*)^2}{qm_2x^{*2}} > p \text{ and } \frac{x^*}{K} + \delta > \frac{qm_2Ex^*}{(m_1E + m_2x^*)^2}. \tag{33}$$

Thus the maximized Hamiltonian H^* is concave in both x and y for all $t \in [0, \infty)$ provided (33) is satisfied. Hence the Arrow sufficiency conditions for infinite time horizon are satisfied [8] under certain constraints.

The generalized Legendre–Clebsch condition for the optimal control problem (22) is trivially satisfied as $\frac{\partial H}{\partial E} = 0$ for all $t \in [0, \infty)$ along the optimal singular solution. Hence from Arrow sufficiency conditions for infinite time horizon and generalized Legendre–Clebsch condition, the singular solution (x^*, y^*, E^*) is a part of optimal solution (piecewise continuous curve) locally. Further, differentiating (23) with respect to t along singular solution together with $(\frac{dx}{dt} = 0)$ and $\frac{d\lambda_1}{dt} = -\frac{\delta Q_2(x)}{Q_1(x)+\delta}e^{-\delta t}$, we get

$$\frac{d}{dt}\frac{dH}{dE} = \left(\frac{qm_2x^2}{(m_1E+m_2x)^2}\left(-p+\frac{Q_2(x)}{Q_1(x)+\delta}\right)+C\right)\delta e^{-\delta t} = 0 \text{ for all } t \in [0, \infty). \tag{34}$$

From (34) we infer that the singular optimal solution is (x^*, y^*, E^*) where x^* is the positive root of the equation

$$\frac{qm_2x^2}{(m_1E + m_2x)^2}\left(-p + \frac{Q_2(x)}{Q_1(x) + \delta}\right) + C = 0$$

which coincides with the fundamental Eq. (31) for the singular solution.

The maximum present value can be found by the evaluation of the performance measure in the obtained optimal values from the previous analysis [20]. In this case

$$J(x^*, E^*) = \int_0^\infty \left(\frac{pq\,x^*}{m_1E^* + m_2x^*} - C\right)E^*e^{-\delta t}dt, \tag{35}$$

this gives

$$J(x^*, E^*) = \frac{\left(\frac{pq\,x^*}{m_1E^*+m_2x^*} - C\right)E^*}{\delta}. \tag{36}$$

Thus,

$$J(x^*, E^*) = \frac{H(x^*, nx^*, E^*, 0)}{\delta}, \tag{37}$$

and the transversality condition

$$\lim_{t\to\infty} e^{-\delta t}H(x^*, y^*, E^*, t) = 0.$$

is trivially satisfied. This result agrees with Michel theorem for discounted autonomous infinite horizon models [8].

Numerical examples: Equation (32) is complex enough to solve for x^* analytically so we consider following numerical examples.

Case (i) $h > c$: For the parameters $\alpha = 0.05, s = 1, q = 2, p = 5, K = 200, r = 5, m_1 = 0.2, m_2 = 0.2, n = 1, C = 1$ satisfying the conditions of the set S_1 (Table 1)

Table 1 Optimal singular equilibrium points for different discount rate δ.

δ	$x^*_{(1)}$	$x^*_{(2)}$	$x^*_{(3)}$	$E^*_{(1)}$	$E^*_{(2)}$	$E^*_{(3)}$	A_4
0.000	38.574	−56.166	−75.741	10.296	−657.040	1188.561	−24.000
0.005	38.609	−56.185	−75.719	10.289	−658.584	1190.968	−24.096
0.050	38.899	−56.358	−75.519	10.231	−672.611	1212.890	−24.958
0.100	39.169	−56.547	−75.303	10.176	−688.514	1237.871	−25.894
0.200	39.562	−56.918	−74.881	10.094	−721.572	1290.229	−27.696

Table 2 Optimal singular equilibrium points for different discount rate δ

δ	$x^*_{(1)}$	$x^*_{(2)}$	$x^*_{(3)}$	$E^*_{(1)}$	$E^*_{(2)}$	$E^*_{(3)}$	A_4
0.000	43.343	Complex	Complex	60.619	Complex	Complex	−4.400
0.005	43.361	Complex	Complex	60.528	Complex	Complex	−4.418
0.050	43.520	Complex	Complex	59.768	Complex	Complex	−4.584
0.100	43.674	Complex	Complex	59.044	Complex	Complex	−4.765
0.200	43.913	Complex	Complex	57.935	Complex	Complex	−5.116

Table 3 Optimal singular equilibrium points for different discount rate δ.

δ	$x^*_{(1)}$	$x^*_{(2)}$	$x^*_{(3)}$	$E^*_{(1)}$	$E^*_{(2)}$	$E^*_{(3)}$	A_4
0.000	39.304	0.695	–	27.362	65.970	–	0.000
0.005	39.337	Complex	Complex	27.329	Complex	Complex	−0.001
0.050	39.611	Complex	Complex	27.054	Complex	Complex	−0.010
0.100	39.868	Complex	Complex	26.797	Complex	Complex	−0.022
0.200	40.247	Complex	Complex	26.419	Complex	Complex	−0.048

Case (ii) $h < c$: For $q = 0.6$ together with above parameters satisfying the conditions of the set S_2 (Table 2)

Case (iii) $h = c$: For $q = 1$ together with above parameter values satisfying the conditions of the set S_3 (Table 3)

Note that $y^*_{(j)} = x^*_{(j)},\ j = 1, \ldots, 3.$ since in each case $n = 1$.

In the above numerical examples we have considered three sets of parameters satisfying the conditions of the sets S_1, S_2 and S_3 respectively. We have solved the Eq. (31) together with steady state Eqs. (15) and (19) for various discount rate δ. From these numerical examples it is clear that we can find the optimum equilibrium for various discount rate δ in various cases. From above three tables we can conclude that there is at least one optimum singular equilibrium point in each case from which $(x^*_{(1)}, y^*_{(1)}, E^*_{(1)})$ is feasible from ecological point of view. Once the optimal singular solution is known then one can easily find the optimal paths (see Fig. 14).

From Fig. 15, we note that at the low population size the harvesting is not profitable as the net profit may become negative. Further, if the parameters lie in the set S_1 (case (i)), then for small population size the net profit (solid curve) increases rapidly than the other two cases while for larger population size the net profit becomes almost constant; the net profit

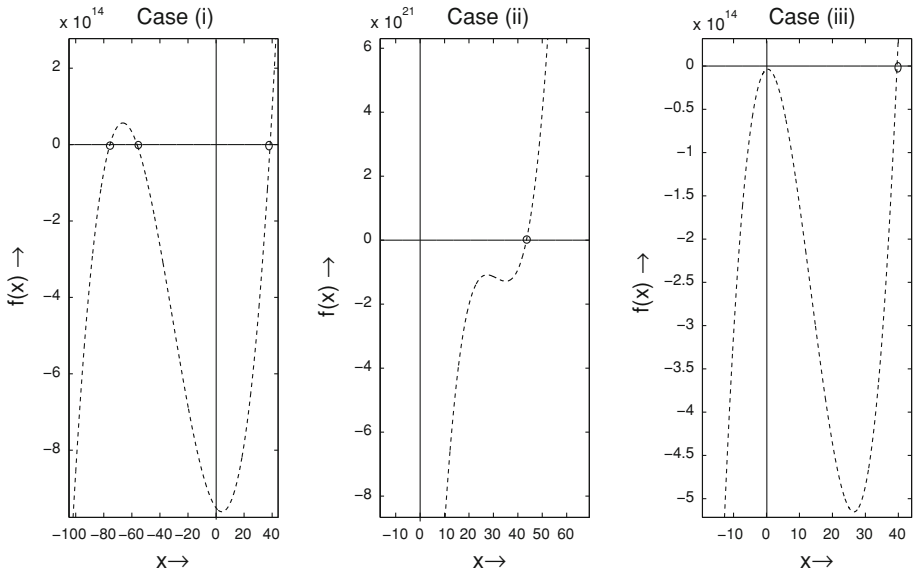

Fig. 14 Number of real roots of (32) for the above three cases with same parameter values defined in the corresponding numerical examples with $\delta = 0.05$ respectively. *Circles* indicate the location of real roots

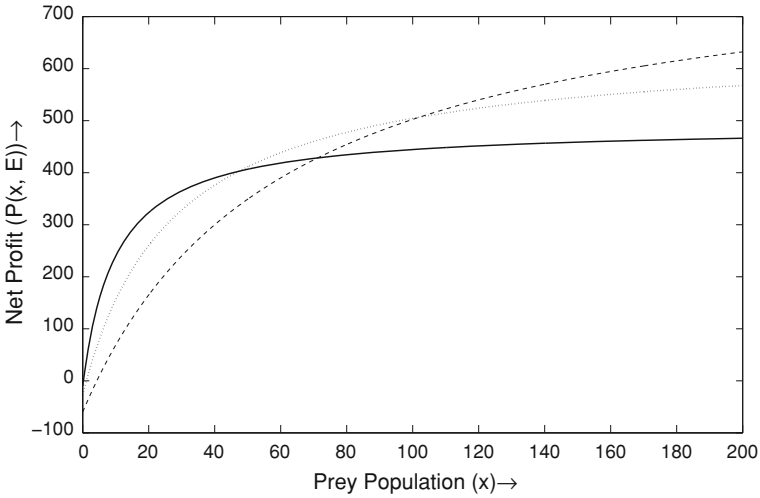

Fig. 15 The net profit for optimum effort together with the corresponding parameter values in each of the above three cases has been plotted on y-axis with respect to the prey population (on x-axis). Here *solid curve* stand for case (i), *dashed curve* stands for case (ii) and *dotted curve* stands for case (iii)

increases at larger population in all the three cases but increases more in the case (iii). Thus we conclude that the case (iii) is more feasible from harvesting point of view.

Discussion

In the present paper, we have considered a Leslie–Gower type predator–prey model with a nonlinear harvesting in prey where the carrying capacity of the predator is proportional

to the number of prey. The model shows rich and varied dynamics. We have discussed the stability of the origin by redefining the system at the origin and then using suitable transformation [11]. The local stability of different steady states have been discussed by using Routh–Hurwitz criterion. We have obtained a bi-stable situation where solutions depend highly on the initial values. We have seen that for a wide range of initial data the system is driven to extinction. More interestingly the model system can have zero, one or two interior equilibria through saddle node bifurcation. The case of bi-stability and existence of more than one interior equilibrium point for the model system are addressed. We have studied the existence of saddle-node bifurcations with the help of Sotomayor's theorem [18]. The local existence of limit cycles in different cases has been observed through Hopf bifurcation and the stability of limit cycles have been examined and validated through numerical simulations by calculating the first Lyapunov number. Exhaustive numerical simulations are carried out to ensure the number of equilibrium points and their stability properties.

We have discussed the conditions for the existence of bionomic equilibrium point of the exploited system. The problem of singular optimal control has been discussed by using Pontryagin's Maximum Principle theory. Here we have attempted the singular optimal control strategy analytically which is a part of optimal harvesting policy. As the control problem satisfies the generalized Legendre–Clebsch Condition [8], we could succeed only up to the singular optimal control strategy. We also have shown that under certain restrictions the Arrow sufficiency conditions [8] for infinite time horizon are satisfied. Hence the singular solution is a part of optimal solution. It is also reported that the control problem satisfies Michel theorem for discounted autonomous infinite horizon. Numerical examples have been given for optimum singular equilibrium points whenever a locally asymptotically equilibrium point exist. Since we have only proceeded up to the singular optimal equilibrium points for the control problem raised therefore the optimal control strategy remains an open problem, i.e., whether the control policy involves both bang-bang control and singular control or it only involves the singular optimal control.

Acknowledgments The work of the first author [R. P. Gupta] is supported by Council of Scientific and Industrial Reseach, India. The authors are thankful to the anonymous reviewers for their valuable suggestions and helpful remarks.

Appendix

Using MAPLE the coefficients of of the cubic polynomial Eq. (32) are given by

$$
\begin{aligned}
A_1 &= 2m_1{}^2psKr\alpha n + 4Kpsr^2m_1{}^2\alpha n + p\delta r^3m_1{}^2 + psr^3m_1{}^2 + m_1{}^2p\delta K^2n^2\alpha^2 + 5m_1{}^2K^2n^2s\alpha^2pr \\
&\quad +2m_1{}^2K^3n^3s\alpha^3p + 3Kp\delta r^2m_1{}^2\alpha n + 2m_1{}^2p\delta Kr\alpha n + K^3p\delta m_1{}^2n^3\alpha^3 + 3K^2p\delta m_1{}^2n^2\alpha^2r \\
&\quad +m_1{}^2psK^2n^2\alpha^2 + m_1{}^2p\delta r^2 + m_1{}^2psr^2, \\
A_2 &= -2m_1{}^2psKr\alpha n - 8Kpsr^2m_1{}^2\alpha n - 5m_1{}^2K^2n^2s\alpha^2pr - 6Kp\delta r^2m_1{}^2\alpha n - 2m_1{}^2p\delta Kr\alpha n \\
&\quad -3K^2p\delta m_1{}^2n^2\alpha^2r + 2Km_1{}^2p\delta^2r\alpha n - K^2m_1Cm_2\delta\alpha^2n^2 - K^2m_1Cm_2s\alpha^2n^2 + 4K^2m_1n^2s\alpha^2pq \\
&\quad +K^2m_1{}^2ps\delta n^2\alpha^2 + 2K^2pq\delta m_1n^2\alpha^2 + 2Km_1pq\delta\alpha n + 2Km_1pqs\alpha n - 2Kns\alpha Cm_2rm_1 \\
&\quad +6Kns\alpha pqrm_1 - 2Km_1Cm_2\delta r\alpha n + 2Km_1{}^2ps\delta r\alpha n + 4Kpq\delta rm_1\alpha n + K^2m_1{}^2p\delta^2n^2\alpha^2 \\
&\quad -3p\delta r^3m_1{}^2 - 3psr^3m_1{}^2 - 2m_1{}^2p\delta r^2 - 2m_1{}^2psr^2 + m_1{}^2p\delta^2r^2 - m_1Cm_2sr^2 - m_1Cm_2\delta r^2 \\
&\quad +m_1{}^2ps\delta r^2 + 2pqsr^2m_1 + 2pq\delta r^2m_1 + 2pqsrm_1 + 2pq\delta rm_1, \\
A_3 &= pq^2\delta + spq^2r + pq^2\delta r + pq^2s + 2Kns\alpha pq^2 + Kpq^2\delta\alpha n + 4Kpsr^2m_1{}^2\alpha n + 3Kp\delta r^2m_1{}^2\alpha n \\
&\quad -2Kns\alpha Cm_2q + 2Km_1pq\delta^2\alpha n - 2Km_1{}^2p\delta^2r\alpha n - KCm_2\delta q\alpha n + 2Kns\alpha Cm_2rm_1 \\
&\quad -6Kns\alpha pqrm_1 + 2Km_1Cm_2\delta r\alpha n - 2Km_1{}^2ps\delta r\alpha n + 2Km_1pqs\delta\alpha n - 4Kpq\delta rm_1\alpha n
\end{aligned}
$$

$$
\begin{aligned}
&+2\,m_1 pqs\delta r + 3\,p\delta r^3 {m_1}^2 + 3\,psr^3 {m_1}^2 + {m_1}^2 p\delta r^2 + {m_1}^2 psr^2 - 2\,{m_1}^2 p\delta^2 r^2 - Cm_2 sq - Cm_2 \delta q \\
&+2\,m_1 Cm_2 sr^2 + 2\,m_1 Cm_2 \delta r^2 - 2\,{m_1}^2 ps\delta r^2 + 2\,m_1 pq\delta^2 r - 4\,pqsr^2 m_1 - 4\,pq\delta r^2 m_1 - Cm_2 \delta qr \\
&-Cm_2 sqr - 2\,pqsrm_1 - 2\,pq\delta rm_1, \\
A_4 = {} & -spq^2 r - pq^2 \delta r - Cm_2 \delta^2 q + pq^2 s\delta + pq^2 \delta^2 - m_1 Cm_2 sr^2 - m_1 Cm_2 \delta r^2 + {m_1}^2 ps\delta r^2 - 2\,m_1 pqs\delta r \\
&+{m_1}^2 p\delta^2 r^2 - 2\,m_1 pq\delta^2 r - psr^3 {m_1}^2 + 2\,pqsr^2 m_1 - p\delta r^3 {m_1}^2 + 2\,pq\delta r^2 m_1 + Cm_2 \delta qr + Cm_2 sqr \\
&-Cm_2 s\delta q.
\end{aligned}
$$

After simplification we get,

$$
A_4 = \left(-pr^3 {m_1}^2 - m_1 \left(-\delta\, pm_1 + Cm_2 - 2\,pq\right) r^2 + q\left(-pq - 2\,\delta\, pm_1 + Cm_2\right) r - \delta\, q\left(-pq + Cm_2\right)\right)(s+\delta).
$$

References

1. Brauer, F., Soudack, A.C.: Stability regions in predator–prey systems with constant-rate prey harvesting. J. Math. Biol. **8**, 55–71 (1979)
2. Brauer, F., Soudack, A.C.: Constant rate harvesting and stocking in predator–prey systems. In: Busenburg, S.N., Cooke, K.L. (eds.) Differential Equation and Applications in Ecology Epidemics and Population Problems, Academic Press, New York (1981)
3. Clark, C.W.: Mathematical Bioeconomics: Te Optimal Management of Renewable Resources. Wiley, New York (1976)
4. Clark, C.W.: Bioeconomic Modelling and Fisheries Management. Wiley, New York (1985)
5. Das, T., Mukherjee, R.N., Chaudhari, K.S.: Bioeconomic harvesting of a prey–predator fishery. J. Biol. Dyn. **3**, 447–462 (2009)
6. Dubey, B., Chandra, P., Sinha, P.: A model for fishery resource with reserve area. Nonlinear Anal. Real World Appl. **4**, 625–637 (2003)
7. Freedman, H.I.: Deterministic Mathematical Models in Population Ecology. Marcel Dekker, New York (1980)
8. Grass, D., Caulkins, J.P., Feichtinger, G., Tragler, G., Behrens, D.A.: Optimal Control of Nonlinear Processes. Springer, Berlin (2008)
9. Haque, M.: Ratio-dependent predator–prey models of interacting populations. Bull. Math. Biol. **71**, 430–452 (2009)
10. Holling, C.S.: The components of predation as revealed by a study of small mammal predation of the European pine sawfly. Can. Entomol. **91**, 293–320 (1959)
11. Jost, C., Arino, O., Arditi, R.: About deterministic extinction in ratio-dependent predator–prey models. Bull. Math. Biol. **61**, 19–32 (1999)
12. Khamis, S.A., Tchuenche, J.M., Lukka, M., Heilio, M.: Dynamics of fisheries with prey reserve and harvesting. Int. J. Comput. Math. **88**(8), 1776–1802 (2011)
13. Krishna, S.V., Srinivasu, P.D.N., Prasad, Kaymakcalan, B.: Conservation of an ecosystem through optimal taxation. Bull. Math. Biol. **60**, 569–584 (1998)
14. Leard, B., Lewis, C., Rebaza, J.: Dynamics of ratio–dependent predator–prey models with non–constant harvesting. Discret. Cont. Dyn. Syst. Ser. S **1**(2), 303–315 (2008)
15. Lenzini, P., Rebaza, J.: Non-constant predator harvesting on ratio-dependent predator–prey models. Appl. Math. Sci. **4**(16), 791–803 (2010)
16. Lin, C.M., Ho, C.P.: Local and global stability for a predator–prey model of modified Leslie–Gower and Holling-Type II with time-delay. Tunghai Sci. **8**, 33–61 (2006)
17. Mena-Lorca, J., González-Olivares, E., González-Yañez, B.: The Leslie–Gower predator–prey model with Allee effect on prey: a simple model with a rich and interesting dynamics. In: Mondaini, R. (ed.) Proceedings of the International Symposium on Mathematical and Computational Biology BIOMAT 2006, E-papers Serviços Editoriais Ltda., R'io de Janeiro, pp. 105–132 (2007).
18. Perko, L.: Differential Equations and Dynamical Systems. Springer, New York (1996)
19. Pontryagin, L.S., Boltyonskii, V.S., Gamkrelidze, R.V., Mishchenko, E.F.: The Mathematical Theory of Optimal Processes. Wiley, New York (1962)
20. Rojas-Palma, A., González-Olivares, E.: Optimal harvesting in a predator–prey model with Allee effect and sigmoid functional response. Appl. Math. Model. **36**, 1864–1874 (2012)
21. Srinivasu, P.D.N.: Bioeconomics of a renewable resource in presence of a predator. Nonlinear Anal. Real World Appl. **2**, 497–506 (2001)
22. Taylor, R.J.: Predation. Chapman and Hall, New York (1984)

23. Zhang, R., Sun, J., Yang, H.: Analysis of a prey–predator fishery model with prey researve. Appl. Math. Sci. **1**, 2481–2492 (2007)
24. Zhang, N., Chen, F., Su, Q., Wu, T.: Dynamic behaviors of a harvesting Leslie–Gower predator–prey model. Discrete Dyn. Nat. Soc. (2011). doi:10.1155/2011/473-949.
25. Zhu, C.R., Lan, K.Q.: Phase portraits, Hopf bifurcations and limit cycles of Leslie–Gower predator–prey systems with harvesting rates. Discrete Contin. Dyn. Syst. Ser. B **14**, 289–306 (2010)